

# A Large Imaging Database and Novel Deep Neural Architecture for Covid-19 Diagnosis

Anastasios Arsenos  
School of Electrical and  
Computer Engineering  
National Technical University Athens  
Email: anarsenos@ails.ece.ntua.com

Dimitrios Kollias  
School of Electronic  
Engineering and Computer Science  
Queen Mary University London  
Email: d.kollias@qmul.ac.uk

Stefanos Kollias  
School of Electrical and  
Computer Engineering  
National Technical University Athens  
Email: stefanos@cs.ntua.gr

**Abstract**—Deep learning methodologies constitute nowadays the main approach for medical image analysis and disease prediction. Large annotated databases are necessary for developing these methodologies; such databases are difficult to obtain and to make publicly available for use by researchers and medical experts. In this paper, we focus on diagnosis of Covid-19 based on chest 3-D CT scans and develop a dual knowledge framework, including a large imaging database and a novel deep neural architecture. We introduce COV19-CT-DB, a very large database annotated for COVID-19 that consists of 7,750 3-D CT scans, 1,650 of which refer to COVID-19 cases and 6,100 to non-COVID-19 cases. We use this database to train and develop the RACNet architecture. This architecture performs 3-D analysis based on a CNN-RNN network and handles input CT scans of different lengths, through the introduction of dynamic routing, feature alignment and a mask layer. We conduct a large experimental study that illustrates that the RACNet network has the best performance compared to other deep neural networks i) when trained and tested on COV19-CT-DB; ii) when tested, or when applied, through transfer learning, to other public databases.

**Index Terms**— medical imaging, COVID-19 diagnosis, COV19-CT-DB database, 3D chest CT scan analysis, RACNet deep neural network, dynamic routing, mask layer, feature alignment.

## I. INTRODUCTION

Various methods have been proposed to diagnose COVID-19, containing a variety of medical imaging techniques, such as analysis of chest x-rays, or CT (computed tomography) scans. In particular, chest 3-D CT images can be used for precise COVID-19 early diagnosis [1], [2]. The target is to detect COVID-19 findings, such as multiple ground-glass opacities, consolidations, and interlobular septal thickening in both lungs, mostly distributed under the pleura.

Machine and deep learning have been used for analyzing CT scans and detecting COVID-19 [3], [4]. Such approaches require large training datasets. A few databases with CT scans have been recently developed [5], [6], [7]. However, some datasets are private and not publicly available [8] [9] [10]. Others are rather small, either in terms of total CT scans, or in terms of COVID-19 annotated CT scans [11] [12] [13]. Moreover, they do not contain volumetric 3-D CT scans (with slices), but only a few CT scan slices or images .

In this paper we present a new very large database, COV19-CT-DB (COVID-19 Computed Tomography Database), including chest 3-D CT scans, aggregated from different hospitals.

In particular, it includes 7,750 3-D CT scans, annotated for COVID-19 infection; 1,650 are COVID-19 cases and 6,100 are non-COVID-19 cases. The 3-D CT scans consist of different numbers of CT slices, ranging from 50 to 700, totalling around 2,500,000 CT slices. Part of the database was successfully used in a recently held Competition [14]. The whole database will be made available to the research community and will be used for research purposes.

We also develop a deep neural architecture able to: i) analyze the 3-D CT scan inputs, ii) effectively handle the problem that each CT scan consists of a different number of CT slices and iii) provide a very high performance, when used on COV19-CT-DB and on other public datasets for COVID-19 diagnosis. RoutingAlignCovidNet (RACNet) is a CNN-RNN (Convolutional Neural Network - Recurrent Neural Network) architecture [15], [16] that is modified to include a feature alignment step and a mask layer that dynamically selects, according to each 3-D input length (i.e., number of slices), the specific RNN outputs to be fed to the dense (fully connected) layers for COVID-19 diagnosis.

The rest of the paper is organized as follows. Section II presents related work, including methods that are considered for comparison purposes in this paper. Section III presents the generated COV19-CT-DB. The RACNet architecture is described in Section IV. Section V includes the experimental study presenting evaluation of the performance of RACNet when trained with COV19-CT-DB and when refined on other public databases. Conclusions and future work are presented in Section VI.

## II. RELATED WORK

A variety of 3-D CNN models have been used for detecting COVID-19 and distinguishing it from other common pneumonia (CP) and normal cases, using volumetric 3-D CT scans [17]. In [18], the authors developed a multi-task architecture consisting of a (common) encoder that takes a 3-D CT scan as input and i) a decoder that reconstructs it; ii) a second decoder that performs COVID lesion segmentation; and iii) a multi-layer perceptron for classification between COVID and non-COVID categories. In [19], a weakly supervised deep learning framework was presented using 3-D CT volumes for COVID-19 classification and lesion localization. A pre-trained UNet was utilized for segmenting the lung region of each CT scan slice; the latter was fed into a 3-D DNN that provided the

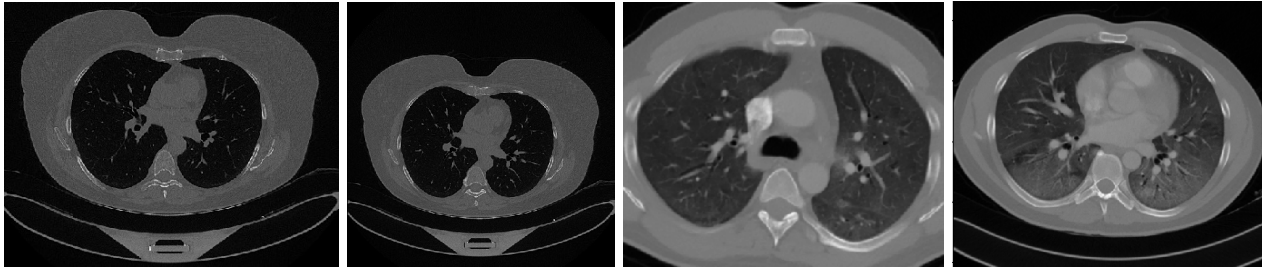


Fig. 1: Four CT scan slices, two from a non-COVID-19 CT scan, on the left and two from a COVID-19 scan, on the right. Bilateral ground glass regions are seen especially in lower lung lobes in the COVID-19 slices.

classification outputs; the COVID-19 lesions were localized by combining the activation regions in the DNN and some connected components in unsupervised way.

In [20] the authors first used 3D models, such as ResNet3D101 and DenseNet3D121, to establish the baseline performance. Then they proposed a differentiable neural architecture search (DNAS) framework to automatically search the 3D DL models for 3D chest CT scan classification and use the Gumbel Softmax technique to improve the search efficiency. This paper has published the training, validation and test datasets that they used in order to have a fair comparison with future works.

### III. THE COV19-CT-DB DATABASE

COV19-CT-DB includes 3-D chest CT scans annotated for existence of COVID-19. Data collection was conducted in the period from September 1 2020 to November 30 2021. It consists of 1,650 COVID and 6,100 non-COVID chest CT scan series, which correspond to a high number of patients (more than 1150) and subjects (more than 2600). Due to the anonymization procedure, no specific patient and subject numbers can be reported.

Annotation of each CT slice has been performed by 4 very experienced (each with over 20 years of experience) medical experts; two radiologists and two pulmonologists. Labels provided by the 4 experts showed a high degree of agreement (around 98%). Each of the 3-D scans includes different number of slices, ranging from 50 to 700. In total, 724,273 slices correspond to the CT scans of the COVID-19 category and 1,775,727 slices correspond to the non COVID-19 category.

Figure 1 shows four CT scan slices, two from a non-COVID-19 CT scan, on the left and two from a COVID-19 scan, on the right. Bilateral ground glass regions are seen especially in lower lung lobes in the COVID-19 slices.

### IV. THE RACNET ARCHITECTURE

#### A. 3-D Analysis and COVID-19 Diagnosis

The input sequence is a 3-D signal, consisting of a series of chest CT slices, i.e., 2-D images, the number of which is varying, depending on the context of CT scanning. The context is defined in terms of various requirements, such as the accuracy asked by the doctor who ordered the scan, the

characteristics of the CT scanner that is used, or the specific subject's features, e.g., weight and age.

The 3-D signal can be handled using a 3-D CNN architecture, such as a 3-D ResNet. However, handling the different input lengths, i.e., the different number of slices that each CT scan contains, can only be tackled in some ad-hoc way, by selecting a fixed input length and removing slices when a larger length is met, or duplicating slices when the input contains a smaller number of slices [21], [22]. The 3-D signal can alternatively be handled using different Multiple Instance Learning methods [23]. Nevertheless, this does not fit our case, as the problem we are dealing is not to identify one or more CT slices that illustrate COVID-19 occurrence; it is to learn doctors' diagnosis making after they have examined the whole 3-D CT scan.

In the proposed approach, we tackle this problem by using RACNet, a CNN-RNN architecture, instead of a 3-D CNN and by including a Mask Layer, following the RNN part, that dynamically selects RNN outputs taking into account the input length, i.e., the number of slices of the currently analyzed CT scan.

Segmentation of each 2-D slice is performed first, so as to detect the lung regions and the resulting segmented image constitutes the input to the CNN.

All input CT scans are padded to have length  $t$  (i.e., consist of  $t$  slices). Then the CNN part performs local, per 2-D slice, analysis, extracting features mainly from the lung regions. The target is to make diagnosis using the whole 3-D CT scan series, similarly to the way medical experts provide the annotation. The RNN part provides this decision, analyzing the CNN features of the whole 3-D CT scan, sequentially moving from slice 0 to slice  $t$ .

As shown in Figure 2, we get RNN features corresponding to each CT slice, from 0 to  $t$ . We then concatenate these features and feed them to the Mask layer. The original (before padding) length  $l$  of the input series is transferred from the input to the Mask layer to inform the routing process. During RACNet training, the routing mechanism performs dynamic selection of the RNN outputs/features. In particular, it selects as many of them as denoted by the length  $l$  of the input series, keeping their values, while zeroing the values of the rest RNN outputs. In this way it is routing only the selected ones into the following dense layer.

This can be done: a) by selecting the first  $l$  RNN outputs, or, b) through an 'alignment' step, i.e., by first placing the  $l$  RNN

outputs in equidistant positions in  $[0, t]$  and by then placing the remaining outputs in the in-between positions; the Mask gets their positions and performs routing of the respective RNN outputs to the following dense layer.

The final output layer then follows that uses a softmax activation function and provides the final COVID-19 diagnosis.

### B. The 'alignment' step

Let us, for example, assume that a maximum input length of 700 CT scan slices is considered. For a specific input CT scan consisting of 50 slices, 650 duplicate slices are inserted so that it is made to contain 700 slices in total. During training, all 700 slices are fed to the CNN-RNN network. In the case where no 'alignment' is performed, the network's output is fed to the Mask layer which: i) zeroes the features corresponding to the 650 duplicate slices (slices 50-699), ii) lets the first 50 features (corresponding to original slices 0-49) keep their values. In the case where 'alignment' is performed, the features extracted from the CNN-RNN part are re-positioned as follows. The features corresponding to the 50 original slices (0-49) are placed in equidistant positions in  $[0, 699]$ . The rest features corresponding to the 650 duplicate slices are placed in the in-between positions. The operation of the Mask layer is the same as when no 'alignment' is performed; it i) zeroes the features corresponding to the 650 duplicate slices (slices 50-699), ii) lets the other 50 features (corresponding to original slices 0-49) keep their values.

In both cases, the 'masked features of CT slices 0-49' and the 'masked features of duplicate CT slices 50-699' are fed to the dense layer that precedes the output layer.

## V. EXPERIMENTAL STUDY

This section describes a set of experiments evaluating the performance of the proposed approach.

At first, we compare the performance of RACNet with the performance of the best methods in an ICCV 2021 competition on COVID-19 diagnosis [14]. A part of COV19-CT-DB composed of 5000 CT scans was used in this Competition. The dataset was split in training, validation and testing sets. The training set contained, in total, 1552 3-D CT scans corresponding to 707 COVID-19 cases and 845 non-COVID-19 cases. The validation set consisted of 374 3-D CT scans, 165 of which represented COVID-19 cases and 209 represented non-COVID-19 cases. Finally the test set included 443 COVID-19 and 3012 non COVID-19 CT scans. We make a comparison of RACNet's performance, trained with the above dataset, to the performance of the three winning methods in the above-mentioned Competition, showing that RACNet outperforms all three methods. Then we evaluate RACNet's performance on another publicly available CT scan database, CC-CCII and show the improved performance when compared to that of the recently published state-of-the-art DNAS framework referenced in Section II [20].

In both cases, we initially performed segmentation of all 3-D CT scans. We used a combination of morphological transforms and a pre-trained U-Net model [24] resulting in a 2D semantic segmentation network. More specifically, for each CT scan, every slice first passed through the pre-trained U-Net

TABLE I: Comparison of RACNet's performance compared to that of state-of-the-art methods on COV19-CT-DB

Method	'macro' F1 Score
ACVLab	88.74
SenticLab.UAIC	90.06
FDVTS_COVID	90.43
RACNet	<b>93.43</b>

model. After all slices of the CT scan were segmented by the U-Net model, there was a checking procedure to assure that all slices were segmented. If a slice had a mask area less than 40 % of the largest mask area of the CT scan, then morphological transforms were used to segment this particular slice. RACNet was trained next, using the segmented training data.

### A. Comparison with best performing methods on COV19-CT-DB

As described in [14], the FDVTS-COVID [25] network achieved the top performance in the ICCV Competition. It included a Periphery-aware Spatial Prediction network, which predicted whether a pixel belonged to the interior of the lung region, as well as the distance to the region boundary. This network was a pre-trained U-Net network with an encoder-decoder architecture; ResNet was adopted as the encoder. Each CT image was at first augmented and then fed into this encoder, generating vector representations. A classifier was trained on top of these representations for COVID-19 classification. Meanwhile, these representations were mapped by a projection network to new representations which were further enhanced in a contrastive learning manner.

The SenticLab.UAIC [26] network ranked second, using an inflated 3D ResNet50 model with non local operations on the second and third layers. Inflated convolutions were obtained by expanding filters and pooling kernels of 2-D ConvNets into 3-D, resulting in learning spatio-temporal feature extractors from 3-D images while using ImageNet architectures and label smoothing. To handle the variable length of CT scans, a sub-sampling technique, or padding, were used for lengths above, or under 128 respectively. During inference, parts of a single CT scan volume were inputted several times in the model; a threshold procedure followed to eliminate some results; final prediction was based on majority voting over remaining results.

The ACVLab [27] network ranked third, based on either slice- level, or 3D volume analysis. In the first case a vision Swin-Transformer was used for single-slice level classification followed by Wilcoxon signed-rank test. In the second case a Within-Slice-Transformer and a Between-Slice-Transformer were used, based on ResNet50 for feature extraction and self-attention for context-encoded features.

We trained the RACNet architecture using the Competition training and validation sets and tested its performance on the test set, similarly to the above three approaches. Table I presents all four methods' performance on the test set, using the official metric of the competition ('macro' F1 score). From this Table it can be easily seen that RACNet provides a superior performance in comparison to the other three approaches.

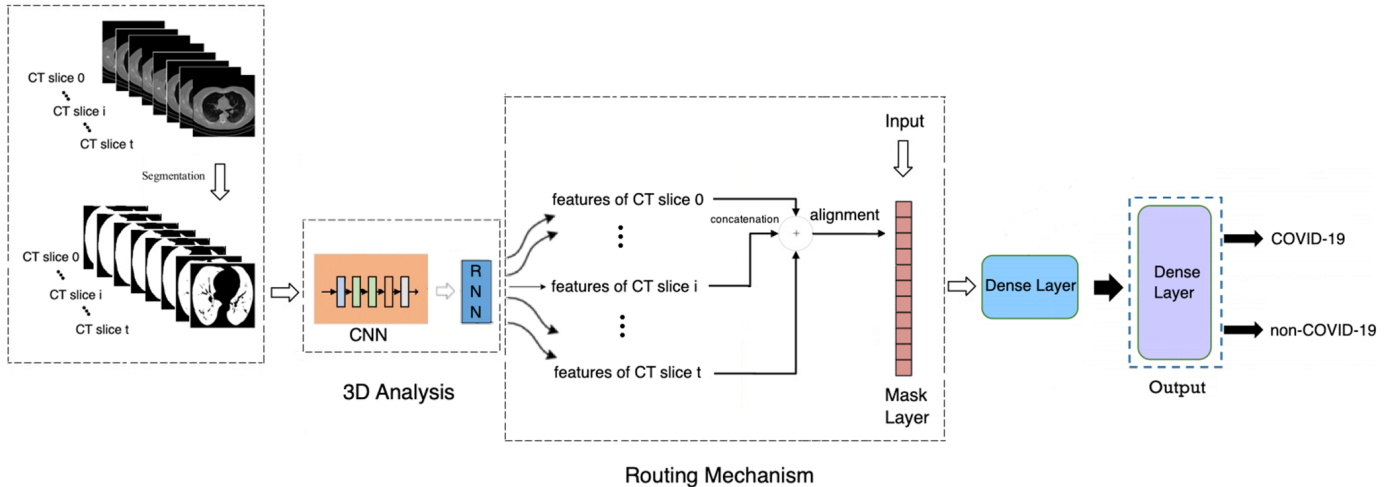


Fig. 2: The proposed Pipeline: A 3-D input composed of, up to  $t$  chest CT slices is processed for COVID-19 diagnosis; 3-D analysis is performed by a CNN-RNN architecture, while a routing mechanism including an 'alignment' step and a Mask Layer handles the varying input length  $t$ . A dense layer follows, preceding the output layer that provides the COVID-19 diagnosis; the neuron outputs of the dense layer are further analyzed through clustering to derive a latent variable model and a related set of anchors that provide further insight into the achieved decision making.

### B. Comparison of Performance of RACNet to 3-D CNNs on CC-CCII Database

In the following we evaluated the performance of the RACNet network on the CC-CCII database [28]. The original CC-CCII dataset contains a total number of 617,775 slices of 6,752 CT scans obtained from 4,154 patients. However, there were some problems with it (i.e., damaged data, non-unified data type, repeated and noisy slices, disordered slices, and non-segmented slices). The authors of [20] published training and test partitions that did not include damaged data and they referred to this version of CC-CCII as 'Clean CC-CCII'.

In order to handle the different number of input CT scan length, the authors of [20] used two slice sampling algorithms: random sampling and symmetrical sampling. Specifically, the random sampling strategy was applied to the training set, which can be regarded as data augmentation, while the symmetrical sampling strategy was performed on the test set to avoid introducing randomness into the testing results. The symmetrical sampling strategy referred to sampling from the middle to both sides at equal intervals. The relative order between slices remained the same before and after sampling.

For a fair comparison we trained, fine-tuned and evaluated RACNet exactly with the same 'Clean-CC-CCII' partitions. In particular: i) we trained the RACNet architecture with the Clean CC-CCII training set and tested its performance on the test set; ii) we trained RACNet initially on the COV19-CT-DB, fine-tuned on the Clean CC-CCII training set and tested its performance on the test set. Table II presents the performance of three state-of-art 3-D CNN networks, as well as of the model described in [20]. It also presents the performance of RACNet in the two above-mentioned contexts. The presented results in Table II indicate that RACNet greatly outperforms all three 3-D CNNs models, as well as the method proposed in [20]. It also indicates that the new COV19-CT-DB database can be used

TABLE II: Comparison of Performance of RACNet to that of 3-D CNNs on the CC-CCII Database

Method	Accuracy score
Resnet3D101	89.62
Densenet3D121	88.97
MCE_18	87.11
COVIDNet3D-L	90.48
RACNet	93.64
RACNet (fine-tuned)	<b>95.33</b>

as an excellent prior for transfer learning and pre-training of deep neural networks for COVID-19 diagnosis in other medical environments.

## VI. CONCLUSIONS AND FUTURE WORK

In this paper we introduced COV19-CT-DB, a new large database of chest 3-D CT scans obtained in various contexts. We have also developed RACNet, a state-of-the-art deep neural architecture that is able to successfully analyze CT scans for COVID-19 diagnosis. We illustrated that RACNet outperforms state-of-the-art 3-D CNNs over the COV19-CT-DB, as well as over the Clean CC-CCII database. Moreover we showed that its performance is further improved when trained on COV19-CT-DB as prior and then refined over Clean CC-CCII database. In future work we will build on the dual generated knowledge, i.e., COV19-CT-DB and RACNet, developing a domain adaptation methodology [29], so as to enrich, in a semi-supervised learning way, the created database with very large numbers of - originally non-annotated - chest 3-D CT scans that will be further aggregated from various medical centres.

## ACKNOWLEDGMENT

We would like to thank GRNET, the Greek National Infrastructures for Research and Technology, for supporting the presented work, through Project "Machaon - Advanced networking and computational services to hospital units in public cloud environment".

## REFERENCES

- [1] R. Alizadehsani, Z. Alizadeh Sani, M. Behjati, Z. Roshanzamir, S. Hussain, N. Abedini, F. Hasanzadeh, A. Khosravi, A. Shoeibi, M. Roshanzamir, P. Moradnejad, S. Nahavandi, F. Khozimeh, A. Zare, M. Panahiazar, U. R. Acharya, and S. M. S. Islam, "Risk factors prediction, clinical outcomes, and mortality in covid-19 patients," *Journal of Medical Virology*, vol. 93, no. 4, pp. 2307–2320, 2021. [Online]. Available: <https://onlinelibrary.wiley.com/doi/abs/10.1002/jmv.26699>
- [2] M. Barstugan, U. Ozkaya, and S. Ozturk, "Coronavirus (covid-19) classification using ct images by machine learning methods," *arXiv preprint arXiv:2003.09424*, 2020.
- [3] S. Wang, B. Kang, J. Ma, X. Zeng, M. Xiao, J. Guo, M. Cai, J. Yang, Y. Li, X. Meng *et al.*, "A deep learning algorithm using ct images to screen for corona virus disease (covid-19)," *European radiology*, pp. 1–9, 2021.
- [4] V. Shah, R. Keniya, A. Shridharani, M. Punjabi, J. Shah, and N. Mehendale, "Diagnosis of covid-19 using ct scan images and deep learning techniques," *Emergency radiology*, pp. 1–9, 2021.
- [5] E. B. Tsai, S. Simpson, M. Lungren, M. Hershman, L. Roshkovan, E. Colak, B. J. Erickson, G. Shih, A. Stein, J. Kalpathy-Cramer *et al.*, "The rsna international covid-19 open annotated radiology database (ricord)," *Radiology*, p. 203957, 2021.
- [6] S. P. Morozov, A. E. Andreychenko, I. A. Blokhin, P. B. Gelezhe, A. P. Gonchar, A. E. Nikolaev, N. A. Pavlov, V. Y. Chernina, and V. A. Gombolevskiy, "Mosmeddata: data set of 1110 chest ct scans performed during the covid-19 epidemic," *Digital Diagnostics*, vol. 1, no. 1, pp. 49–59, 2020.
- [7] P. Afshar, S. Heidarian, N. Enshaei, F. Naderkhani, M. J. Rafiee, A. Oikonomou, F. B. Fard, K. Samimi, K. N. Plataniotis, and A. Mohammadi, "Covid-ct-md: Covid-19 computed tomography (ct) scan dataset applicable in machine learning and deep learning," *arXiv preprint arXiv:2009.14623*, 2020.
- [8] L. Li, L. Qin, Z. Xu, Y. Yin, X. Wang, B. Kong, J. Bai, Y. Lu, Z. Fang, Q. Song, K. Cao, D. Liu, G. Wang, Q. Xu, X. Fang, S. Zhang, J. Xia, and J. Xia, "Using artificial intelligence to detect covid-19 and community-acquired pneumonia based on pulmonary ct: Evaluation of the diagnostic accuracy," *Radiology*, vol. 296, no. 2, pp. E65–E71, 2020, pMID: 32191588. [Online]. Available: <https://doi.org/10.1148/radiol.2020200905>
- [9] Y. Song, S. Zheng, L. Li, X. Zhang, X. Zhang, Z. Huang, J. Chen, R. Wang, H. Zhao, Y. Chong, J. Shen, Y. Zha, and Y. Yang, "Deep learning enables accurate diagnosis of novel coronavirus (covid-19) with ct images," *IEEE/ACM Transactions on Computational Biology and Bioinformatics*, vol. 18, no. 6, pp. 2775–2780, 2021.
- [10] A. Borakati, A. Perera, J. Johnson, and T. Sood, "Diagnostic accuracy of x-ray versus ct in covid-19: a propensity-matched database study," *BMJ Open*, vol. 10, no. 11, 2020. [Online]. Available: <https://bmjopen.bmj.com/content/10/11/e042946>
- [11] X. Yang, X. He, J. Zhao, Y. Zhang, S. Zhang, and P. Xie, "Covid-ct-dataset: a ct image dataset about covid-19," *arXiv preprint arXiv:2003.13865*, 2020.
- [12] E. B. Tsai, S. Simpson, M. P. Lungren, M. Hershman, L. Roshkovan, E. Colak, B. J. Erickson, G. Shih, A. Stein, J. Kalpathy-Cramer, J. Shen, M. Hafez, S. John, P. Rajiah, B. P. Pogatchnik, J. Mongan, E. Altinmakas, E. R. Ranschaert, F. C. Kitamura, L. Topff, L. Moy, J. P. Kanne, and C. C. Wu, "The rsna international covid-19 open radiology database (ricord)," *Radiology*, vol. 299, no. 1, pp. E204–E213, 2021, pMID: 33399506. [Online]. Available: <https://doi.org/10.1148/radiol.2021203957>
- [13] E. Soares, P. Angelov, S. Biaso, M. H. Froes, and D. K. Abe, "Sars-cov-2 ct-scan dataset: A large dataset of real patients ct scans for sars-cov-2 identification," *medRxiv*, 2020. [Online]. Available: <https://www.medrxiv.org/content/early/2020/05/14/2020.04.24.20078584>
- [14] D. Kollias, A. Arsenos, L. Soukissian, and S. Kollias, "Mia-cov19d: Covid-19 detection through 3-d chest ct image analysis," in *Proceedings of the IEEE/CVF International Conference on Computer Vision*, 2021, pp. 537–544.
- [15] D. Kollias, A. Tagaris, A. Stafylopatis, S. Kollias, and G. Tagaris, "Deep neural architectures for prediction in healthcare," *Complex & Intelligent Systems*, vol. 4, no. 2, pp. 119–131, 2018.
- [16] F. Caliva, F. S. De Ribeiro, A. Mylonakis, C. Demazi'ere, P. Vinai, G. Leontidis, and S. Kollias, "A deep learning approach to anomaly detection in nuclear reactors," in *2018 International joint conference on neural networks (IJCNN)*. IEEE, 2018, pp. 1–8.
- [17] Y. Li, X. Pei, and Y. Guo, "A 3d cnn classification model for accurate diagnosis of coronavirus disease 2019 using computed tomography images," *medRxiv*, 2021.
- [18] A. Amyar, R. Modzelewski, H. Li, and S. Ruan, "Multi-task deep learning based ct imaging analysis for covid-19 pneumonia: Classification and segmentation," *Computers in Biology and Medicine*, vol. 126, p. 104037, 2020.
- [19] X. Wang, X. Deng, Q. Fu, Q. Zhou, J. Feng, H. Ma, W. Liu, and C. Zheng, "A weakly-supervised framework for covid-19 classification and lesion localization from chest ct," *IEEE transactions on medical imaging*, vol. 39, no. 8, pp. 2615–2625, 2020.
- [20] X. He, S. Wang, X. Chu, S. Shi, J. Tang, X. Liu, C. Yan, J. Zhang, and G. Ding, "Automated model design and benchmarking of 3d deep learning models for covid-19 detection with chest ct scans," 2021. [Online]. Available: <https://arxiv.org/abs/2101.05442>
- [21] D. Kollias, N. Bouas, Y. Vlaxos, V. Brillakis, M. Seferis, I. Kollia, L. Sukissian, J. Wingate, and S. Kollias, "Deep transparent prediction through latent representation analysis," *arXiv preprint arXiv:2009.07044*, 2020.
- [22] D. Kollias, Y. Vlaxos, M. Seferis, I. Kollia, L. Sukissian, J. Wingate, and S. D. Kollias, "Transparent adaptation in deep medical image diagnosis," in *TAILOR*, 2020, pp. 251–267.
- [23] Z. Han, B. Wei, Y. Hong, T. Li, J. Cong, X. Zhu, H. Wei, and W. Zhang, "Accurate screening of covid-19 using attention-based deep 3d multiple instance learning," *IEEE transactions on medical imaging*, vol. 39, no. 8, pp. 2584–2594, 2020.
- [24] R. Azad, M. Asadi-Aghbolaghi, M. Fathy, and S. Escalera, "Bi-directional convlstm u-net with densley connected convolutions," in *Proceedings of the IEEE/CVF International Conference on Computer Vision (ICCV) Workshops*, Oct 2019.
- [25] J. Hou, J. Xu, R. Feng, Y. Zhang, F. Shan, and W. Shi, "Cmc-cov19d: Contrastive mixup classification for covid-19 diagnosis," in *Proceedings of the IEEE/CVF International Conference on Computer Vision (ICCV) Workshops*, October 2021, pp. 454–461.
- [26] R. Miron, C. Moisii, S. Dinu, and M. Breaban, "Covid detection in chest cts: Improving the baseline on cov19-ct-db," *arXiv*, 2021. [Online]. Available: <https://arxiv.org/abs/2107.04808>
- [27] C.-C. Hsu, G.-L. Chen, and M.-H. Wu, "Visual transformer with statistical test for covid-19 classification," *arXiv*, 2021. [Online]. Available: <https://arxiv.org/abs/2107.05334>
- [28] K. Zhang, X. Liu, J. Shen, Z. Li, Y. Sang, X. Wu, Y. Zha, W. Liang, C. Wang, K. Wang, L. Ye, M. Gao, Z. Zhou, L. Li, J. Wang, Z. Yang, H. Cai, J. Xu, L. Yang, W. Cai, W. Xu, S. Wu, W. Zhang, S. Jiang, L. Zheng, X. Zhang, L. Wang, L. Lu, J. Li, H. Yin, W. Wang, O. Li, C. Zhang, L. Liang, T. Wu, R. Deng, K. Wei, Y. Zhou, T. Chen, J. Y.-N. Lau, M. Fok, J. He, T. Lin, W. Li, and G. Wang, "Clinically applicable ai system for accurate diagnosis, quantitative measurements, and prognosis of covid-19 pneumonia using computed tomography," *Cell*, vol. 181, no. 6, pp. 1423–1433.e11, 2020. [Online]. Available: <https://www.sciencedirect.com/science/article/pii/S0092867420305511>
- [29] D. Kollias, M. Yu, A. Tagaris, G. Leontidis, A. Stafylopatis, and S. Kollias, "Adaptation and contextualization of deep neural network models," in *2017 IEEE symposium series on computational intelligence (SSCI)*. IEEE, pp. 1–8.